Smart Structures and Systems, *Vol. 20, No. 2 (2017) 175-180*
DOI: https://doi.org/10.12989/sss.2017.20.2.175

Grouting compactness monitoring of concrete-filled steel tube arch bridge model using piezoceramic-based transducers

Qian Feng[1,2], Qingzhao Kong*[3], Jie Tan[1,2] and Gangbing Song[3,4]

[1]Key Laboratory of Earthquake Geodesy, Institute of Seismology, China Earthquake Administration, Wuhan, 430071, China
[2]Wuhan Institute of Earthquake Engineering, Wuhan, 430071, China
[3]Department of Mechanical Engineering, University of Houston, 4800 Calhoun, Houston, 77204, USA
[4]School of Civil and Hydraulic Engineering, Dalian University of Technology, Dalian, Liaoning 116024, China

(Received November 28, 2016, Revised March 30, 2017, Accepted April 6, 2017)

Abstract. The load-carrying capacity and structural behavior of concrete-filled steel tube (CFST) structures is highly influenced by the grouting compactness in the steel tube. Due to the invisibility of the grout in the steel tube, monitoring of the grouting progress in such a structure is still a challenge. This paper develops an active sensing approach with combined piezoceramic-based smart aggregates (SA) and piezoceramic patches to monitor the grouting compactness of CFST bridge structure. A small-scale steel specimen was designed and fabricated to simulate CFST bridge structure in this research. Before casting, four SAs and two piezoceramic patches were installed in the pre-determined locations of the specimen. In the active sensing approach, selected SAs were utilized as actuators to generate designed stress waves, which were detected by other SAs or piezoceramic patch sensors. Since concrete functions as a wave conduit, the stress wave response can be only detected when the wave path between the actuator and the sensor is filled with concrete. For the sake of monitoring the grouting progress, the steel tube specimen was grouted in four stages, and each stage held three days for cement drying. Experimental results show that the received sensor signals in time domain clearly indicate the change of the signal amplitude before and after the wave path is filled with concrete. Further, a wavelet packet-based energy index matrix (WPEIM) was developed to compute signal energy of the received signals. The computed signal energies of the sensors shown in the WPEIM demonstrate the feasibility of the proposed method in the monitoring of the grouting progress.

Keywords: grouting compactness monitoring; concrete-filled steel tube arch bridge; piezoceramic-based transducers; smart aggregates; active sensing approach

1. Introduction

In recent years, Concrete-Filled Steel Tube (CFST) structures, which exhibit the advantages of both steel and concrete, have been widely employed in civil infrastructures, such as subway stations, high-rise buildings, and arch bridges, due to their performance of high load-carrying capability, good ductility, convenience and economy in construction. Fig. 1 shows two examples of CFST arch bridges. In practice, incomplete cement grouting of CFST structures can cause defect in concrete core and interface debonding, which may reduce the structural integrity, load-carrying capability, and service life, and even cause structural failure (Su 2009). Due to the invisibility of the internal grout condition during grouting process, monitoring of the grouting process using traditional inspection methods is very difficult.

With the recent advances in structural health monitoring (Yi *et al.* 2013, Lai *et al.* 2016, Yi *et al.* 2015, Kong *et al.* 2016, Feng *et al.* 2013, Ni *et al.* 2010, Ni *et al*. 2012, Liu *et al*. 2016, Zou *et al*. 2014, Ye *et al.* 2016), monitoring of the structural health of CFST structures receive attentions from both practicing engineers and academic researchers. The current methods include knocking technology (Chen 2011), ultrasonic detection (Lu *et al*. 2011, Liu 2004), and fiber Bragg grating detection technique (Ni et al. 2009, Lin *et al.* 2004), have been reported. Xu *et al.* (2017), Xu *et al.* (2012), Xu *et al.* (2017) conducted both the numerical ad experimental studies to reveal the debonding mechanisms and detect the debonding damage for different types of CFSTs using piezoceramic based transducers. Liu *et al.* (2004) proposed an ultrasonic quality detection method to monitor the grouting quality of concrete core in a concrete-filled steel arch bridge. The effectiveness of the proposed technique was verified by a field detection of The North Rail Station Bridge in Shenzhen city. For the detection of concrete quality between the jacket and the concrete of fiber reinforced polymer-wrapped concrete structure, Feng *et al*. (2002) developed an electromagnetic (EM) imaging technique based on the reflection of a continuous EM waves and the reflection from the layered FRP-adhesive-concrete medium. In addition, the electro-mechanical impedance (EMI) technique was also employed to diagnose the surface defects and damage between the steel and concrete (Liang *et al.* 2016).

With the proven advantages of the availability in different shapes, wide bandwidth, low price, and the ability of being employed as both actuators and sensors of the

*Corresponding author
E-mail: qzkong123@gmail.com

http://www.techno-press.com/journals/sss&subpage=7
ISSN: 1738-1584 (Print), 1738-1991 (Online)

piezoelectric materials, Lead Zirconate Titanate (PZT)-based transducers have been widely recognized as one of the most promising tools for structural health monitoring (SHM) (Siu *et al.* 2014, Ruan *et al*. 2015, Yao *et al.* 2016, Zhang *et al*. 2016, Zeng *et al.* 2015, Xiao *et al.* 2015). In order to overcome the fragility of PZT materials, Song *et al.* (2007), Song *et al.* (2007), Song *et al.* (2008) developed a PZT-based multi-functional smart aggregate (SA), which can be embedded into the concrete structure in a distributed fashion. For example, an active interface condition monitoring approach was proposed and experimentally verified by Xu *et al*. (2013) to detect the debonding damage for CFST by the use of embedded SAs in concrete as actuator and PZT patches mounted on the surface of the steel tube as sensors. Zou *et al.* (2014), Zou *et al.* (2014), Liu *et al*. (2013) tested the performance of SAs in water environment and applied the SA based active sensing approach to monitor the water seepage in concrete structures. Jiang *et al*. (2016) presented a stress wave-based active sensing approach using piezoceramic transducers to monitor the grouting compactness in a post-tensioning tendon duct in real-time. The grouting compactness can be successfully evaluated by using both the time domain analysis and energy analysis. In addition, Feng *et al.* (2015) performed wavelet packet-based energy analysis with SAs to detect cracks and determine the further leakage of a concrete pipeline specimen based on the stress wave energy attenuation change through cracks and cracks filled with water. However, the SA-based active sensing approach has never been reported to monitor the grouting progress for CFST bridge structures.

In this paper, an active sensing approach with combined SAs and piezoceramic patches was proposed to monitor the grouting progress. A small-scale steel tube was designed and fabricated to simulate the CFST bridge structure. A sensor network, including four SAs and two PZT patches, was deployed in the specimen.

Fig. 1 Photos of CFST arch bridges

The specimen was grouted through a reserved grouting hole in four stages, and each stage holds three days for cement drying. In the experiments, designed stress wave propagated between SA and SA or SA and piezoceramic patch by using the active sensing approach. Since concrete functions as a wave conduit, the stress wave response can be only detected when the wave path between the selected actuator and sensor is filled with concrete. The change of the sensor signal amplitude in grouting process can be observed in time domain. Further, a wavelet packet-based energy index matrix (WPEIM) was developed to compute energy of the received signal. The proposed WPEIM is capable of providing computed signal energies of the sensors in different grouting stages which can be used to monitor the grouting progress.

2. Piezoceramic-based transducers

Piezoelectricity can be simply expressed as, when an electric field is applied on the piezoelectric material, it will generate strain of stress, and vice versa. The most popular piezoceramic material, Lead Zirconate Titanate (PZT), exhibits high piezoelectricity and has been researched in many applications of structural health monitoring in recent years. Since a PZT patch is fragile and can be easily damaged, a smart aggregate is designed by sandwiching the fragile PZT patch between two marble protections (Hou *et al.* 2012). The marble protections ensure the functionality of SAs when being used as embedded transducers in concrete structures. Research of SA-based structural health monitoring have been conducted for years (Son *et al.* 2007, Son *et al*. 2007). Figs. 2 (a) and 2(b) shows respectively an electrical isolated PZT patch and an SA. Both transducers are connected with BNC connectors. In this research, distributed PZT patches and SAs are mounted on the surface of the steel tube and embedded in the concrete, respectively.

(a)

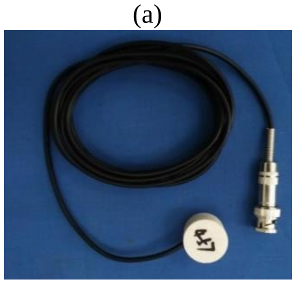

(b)

Fig. 2 Photos of a PZT patch and a smart aggregate: (a) A PZT patch with a BNC connector and (b) AnSA with a BNC connector

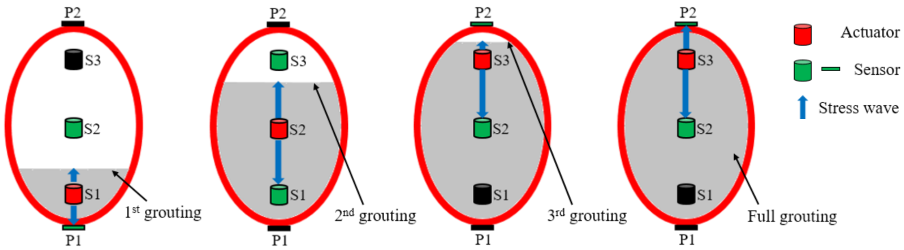

Fig. 3 Detection schematic of active sensing based grouting compactness monitoring

3. Detection principles

3.1 Active sensing approach

An active sensing approach with combined PZT patches and SAs is developed in monitoring the grouting compactness of the CFST bridge structure. Due to the piezoelectricity, either a PZT patch or a SA can be used as an actuator or a sensor. In the activing sensing approach, a designed swept sine signal is applied to the selected actuator, generating a stress wave that propagates in the concrete. Other sensors will detect the wave response. Since the stress wave can hardly propagate in air, sensor cannot receive a meaningful signal until the wave path between the actuator and the sensor is filled with concrete. Fig. 3 gives detection schematics of active sensing based grouting compactness monitoring used in this research. In Fig. 3, S*i*(*i*=1, 2, 3) represents the *i*th SA and P*i*(*i*=1, 2, 3) represents the *i*th PZT patch. The three SAs (S1, S2, and S3) were pre-installed in the steel tube before grouting and the two PZT patches (P1, P2) were mounted on the outer surface of the steel tube with epoxy resin. The grouting progress, or the height of the grout, can be evaluated by using certain selected actuator-sensor pairs, as shown in Fig. 3. As an example of the first grouting stage, only the sensor (P1) can detect wave response when S1 is used as an actuator. However, neither S2 nor S3 can receive any signal in this stage. Similarly, when the second grouting stage is completed, S1can detect wave response but S3 cannot when S2 is used as an actuator. It can be seen that the fulfillment of the grouting can be determined when P2 sensor starts to detect wave response form the actuator S3.

3.2 Wavelet Packet-based Energy Index Matrix (WPEIM)

Wavelet packet-based analysis have been utilized to report structural damage (Siu *et al*. 2014). In this research, a wavelet packet-based energy index matrix was developed to monitor the grouting progress. In each measurement using active sensing approach, the sensor signal X can be decomposed by n-level wavelet packet decomposition into 2^n signal sets (Yao *et al.* 2015). The total energy of each received signal can be further computed by the summation of all the signal sets (Jiang *et al.* 2016). Based on the computed energy of the signal, the proposed wavelet packet-based energy index matrix can be defined as

$$M_{m\times n}=[E_{i,j}]$$

where the matrix element $E_{i,j}$ represents the computed sensor signal energy of the ith actuator at the time of the jth measurement (i=1,2,…,m and j=1,2,…,n). In this research, the proposed three-dimensional energy index matrix help to indicate the sensor signal energy at different locations of the specimen in different grouting stages. By comparing the sensor energies among distributed sensors at the same measurement, the grouting progress can be monitored.

4. Experimental setup and procedures

4.1 Specimen and sensor location

A small-scale steel tube specimen was designed and fabricated to simulate the CFTB bridge structure. The construction material of the steel tube is Steel Q235. Three grouting holes were reserved for cement grouting. In this research, cement was filled only in the left side of the specimen using the left grouting hole. All the SAs were bonded on a supporting wood stick with epoxy resin before putting inside the steel tube specimen, as shown in Fig. 4 (a). PZT patches were directly mounted at pre-determined locations on the outer surface of the steel tube using epoxy resin. Fig. 4(b) shows amounted PZT patch and the installed SAs. The dimensions of the steel tube specimen and the detailed sensor location are shown in Fig. 5.

4.2 Experimental setup and procedures

Fig. 6 shows the experimental setup, including the small-scale steel tube specimen, installed transducers, and data acquisition system. The operating sampling frequency of the data acquisition system is 2 MS/s. In the experiment, the left side of the steel tube specimen was grouted through the grouting hole by four times, as shown in Fig. 3(a). The grouting cement is C40 which is a typical type of construction concrete with the compressive strength of 40 Mpa. Shortly after grouting, compaction was performed by tapping a rubber mallet at the exterior of the steel tube to remove the voids from the cement. In each grouting stage, the active sensing based measurements were performed in the selected four sensor channels that include S1-P1, S1-S2, S2-S3, S3-P2. For each sensor channel, the first symbol is the actuator and the second symbol is the sensor. In each test of the sensor channels, a swept sine signal was applied to the actuator generating a designed stress wave, while the corresponding sensor detected the wave response. Due to the response spectrum of the SA, the frequency range of 100 Hz-300 kHz was applied in this research. The details of the excitation signal can be found in Table 1. To conduct the staged concrete casting, the each grouting stage holds three days for cement drying. The measurements conducted at the 3rd day of each grouting stage.

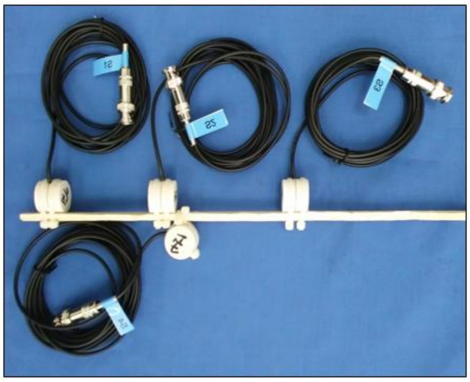

(a)

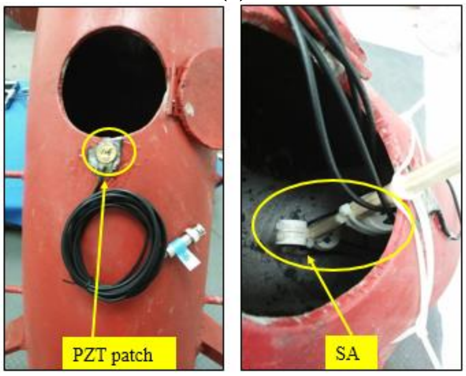

(b)

Fig. 4 Transducer installation: (a) SAs supported with a wood stick and (b) A photo of mounted PZT patch and installed SAs

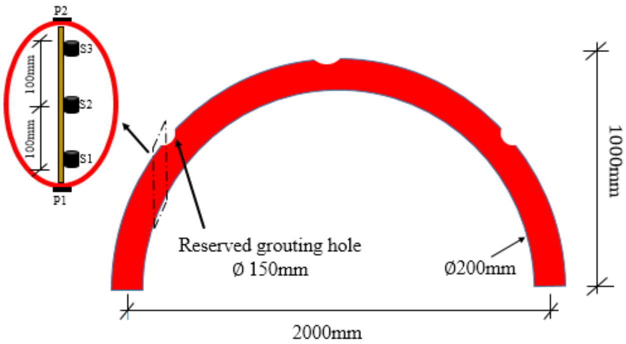

Fig. 5 Dimensions of the steel tube specimen and the location of the transducers

Table 1 Details of the swept sine signal

Amplitude	10 V
Frequency range	100 Hz-300 kHz
Period	1s

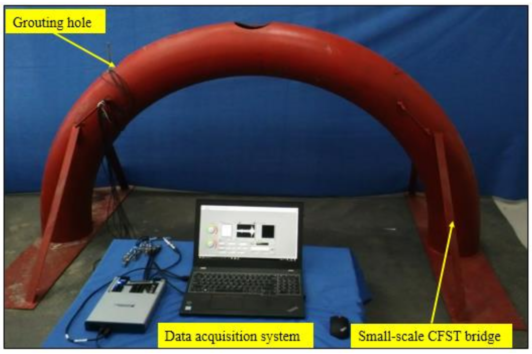

Fig. 6 Experimental setup

5. Test results and discussions

5.1 Received Sensor signal in time domain

Fig. 7 gives one period of the signal response of S1-P1 in two cases, including no grout and the third day after the first grouting. When the steel tube is not grouted, the guided stress wave cannot propagate through S1 to P1. Therefore, no signal can be detected from P1, as shown in Fig. 7(a). When the first grouting was completed, the concrete was filled between S1 and P1, as shown in Fig. 2(a). P1 started to detect stress wave response from S1, and the received signal at the third day after the first grouting is shown in Fig. 7(b). The obvious change of the received signal in the time domain clearly demonstrates that the proposed active sensing approach can detect if there is concrete being filled between the actuator-sensor pair. To monitor the grouting progress by the distributed SAs and PZT patches, the results of the developed MPEIM was presented in the next section.

5.2 Wavelet packet-based energy index matrix (WPEIM)

The results of using the developed WPEIMs are shown in Fig. 8, representing vertically distributed actuator-sensor channels, respectively. Based on the energy computation of the sensor signal using wavelet technique, the energy values of the distributed sensors at different grouting stages are presented. Four vertically distributed actuator-sensor channels, including S1-P1, S1-S2, S2-S3, S3-P2, are shown in Figs. 8(a) and 8(b), respectively. The WPEIM clearly indicates that all the sensors cannot receive any signal response before grouting since the stress wave cannot propagate through the hollow tube. When the first grouting was completed, none of the sensors but P1 can receive signal from the corresponding actuator S1 since the actuator-sensor channel S1-P1 was filled with concrete in the first grouting stage. When the second grouting stage was completed, S2 begins to detect wave response from S1. Since concrete also exists in the channel S1-P1, WPEIM continuously reports sensor signal energy of P1. The same trend can be also found in the third grouting stage and the fourth grouting stage (full grouting). Since P2 was mounted on the top surface of the steel tube, the appearance of the energy values of P2 in WPEIM implies the fulfillment of the cement grouting.

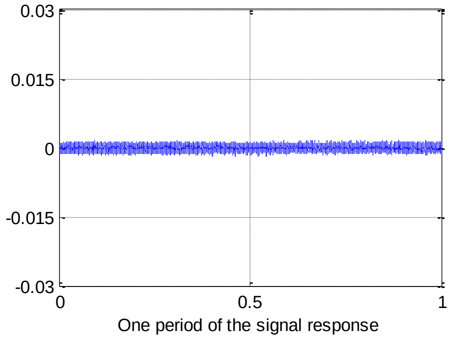

(a) No grout

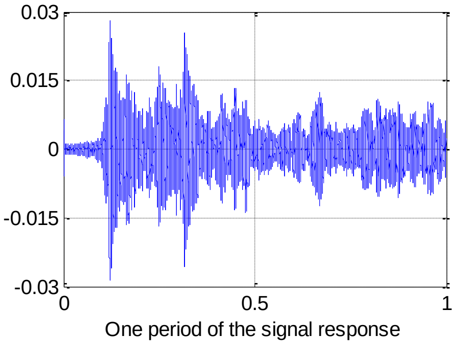

(b) the 3rd day after 1st grouting

Fig. 7 One period of the signal response of S1-P1

It can also been seen that the signal energy of each sensor increases as the grouting continues. The reason is the increase of the concrete strength during hydration will help to propagate the stress wave (Kong *et al*. 2013), resulting in the increase of the received signal amplitude. In Fig. 8, by the influence of the distance between the actuator to the sensor and the different sensor types (SA and PZT patch), the energy values between S1-P1, S3-P2 and S1-S2, S2-S3 in the same grouting stage are different. Another possible reason for the distinct values in the same grouting stage is the concrete material exhibits nonlinear properties which may cause the nonlinear stress wave propagation between transducers.

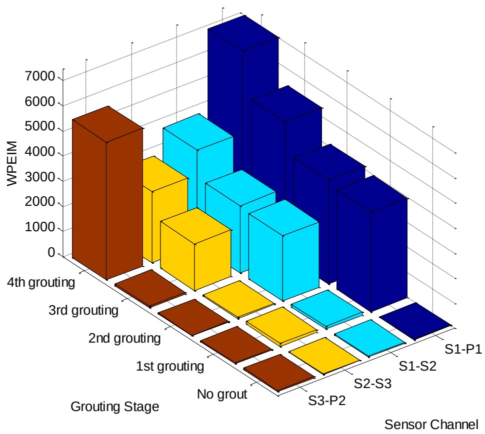

Fig. 8 Results of WPEIM-Vertically distributed sensor channels: S1-P1, S1-S2, S2-S3, S3-P2

5.3 Discussion

As shown in Section 5.2, the grouting progress can be effectively monitored through the vertically distributed transducers. In addition, the fulfillment of the cement grouting can be also detected when the energy values of P2 in WPEIM increase. However, the proposed approach still has some limitations. Firstly, the proposed method can only report the compactness of limited area based on the location of the distributed transducers. Evaluation of the general compactness condition of large-scale CFST structure still remains further improvement of the current approach. Secondly, the installation of the SAs in the large-scale arch bridge before grouting may be a complex procedure that needs to be addressed.

6. Conclusions

In this research, an active sensing approach with combined Smart Aggregates (SAs) and PZT patches is proposed to monitor the grouting progress of a CFST bridge structure. The developed WPEIM can successfully indicate the degree of the grouting completeness based on the distributed transducers. When WPEIM begins to report signal energy received by the PZT sensor mounted on the top surface of the steel tube, the fulfillment of the grouting is accomplished. In addition, the local compactness between steel tube and concrete core can be detected by the distributively surface mounted PZT sensors. However, implementation of the proposed method into practical applications of compactness monitoring in large-scale structures still remains many difficulties, including improvement of the detection range, SA installation, wire protection, which are considered as authors' future work.

Acknowledgments

This work was partially supported by the Major State Basic Research Development Program of China (973 Program, grant number 2015CB057704), National Natural Science Foundation of China (grant number51608493, 51478080 and 51278084), Director's Foundation of Institute of Seismology, China Earthquake Administration (Grant number IS201626258, IS201626268 and IS201616250) and Ministry of Human Resources and Social Security, People's Republic of China. The authors would like to thank for these financial supports.

References

Chen, L. (2011), "Debonding defect detection for concrete filled steel tubular using knocking technique", *China Concrete*, **1**, 54-56.

Feng, M.Q., Flaviis, F.D. and Kim, Y.J. (2002), "Use of microwaves for damage detection of fiber reinforced polymer-wrapped concrete structures", *J. Eng. Mech. - ASCE*, **128**(2), 172-183.

Feng, Q., *et al*. (2015), "Crack detection and leakage monitoring on reinforced concrete pipe", *Smart Mater. Struct.*, **24**(11),

115020.
Feng, Q., *et al*. (2013), "Design of remote real time monitoring system based on GPRS for railway roadbed subsidence", *J. Geodesy Geodynam*, **6**, 155-157.
Hou, S., Zhang, H.B. and Ou, J.P. (2012), "A PZT-based smart aggregate for compressive seismic stress monitoring", *Smart Mater. Struct.*, **21**(10), 105035.
Jiang, T., *et al*. (2016), "Monitoring of grouting compactness in a post-tensioning tendon duct using piezoceramic transducers", *Sensors*, **16**(8), 1343.
Kong, Q., Hou, S., Ji, Q., Mo, Y.L. and Song, G. (2013), "Very early age concrete hydration characterization monitoring using piezoceramic based smart aggregates", *Smart Mater. Struct*., **22**(8), 085025.
Kong, Q., Robert, R.H., Silva, P. and Mo, Y.L. (2016), "Cyclic crack monitoring of a reinforced concrete column under simulated pseudo-dynamic loading using piezoceramic-based smart aggregates", *Appl. Sci*., **6**(11), 341.
Lai, T., Yi, T.H. and Li, H.N. (2016), "Parametric study on sequential deconvolution for force identification", *J. Sound Vib*., **377**, 76-89.
Liang, Y., *et al*. (2016), "Bond-slip detection of concrete-encased composite structure using electro-mechanical impedance technique", *Smart Mater. Struct*., **25**(9).
Lin Y.B., *et al*. (2004), "The utilization of fiber Bragg grating sensors to monitor high performance concrete at elevated temperature", *Smart Mater. Struct*., **13**(4), 784-790.
Liu, Q. (2004), "Compactness detection research for concrete filled steel tube arch bridge using ultrasonic technique", *NDT*, **2**, 13-15.
Liu, T., Huang, Y., Zou, D., Teng, J. and Li, B. (2013), "Exploratory study on water seepage monitoring of concrete structures using piezoceramic based smart aggregates", *Smart Mater. Struct*., **22**(6), 065002.
Liu, T., Zou, D., Du, C. and Wang, Y. (2016), "Influence of axial loads on the health monitoring of concrete structures using embedded piezoelectric transducers", *Struct. Health Monit*., 1475921716670573.
Liu, Y., Zhang Y. and Zou Z. (2004), "Study of ultrasonic detection and evaluation for the deficiency of concrete-filled steel tube arch bridge", *J. Northern Jiaotong Univ*., **4**, 54-57.
Lu, X., Xu, R. and Wang, G. (2011), "Common defects in the concrete-filled steel tube and its detection methods", *Constr. Technol*., (S1), 46-48.
Ni, Y.Q., *et al*. (2009), "Technology innovation in developing the structural health monitoring system for Guangzhou New TV Tower", *Struct. Control Health Monit*., **1**(16), 73-98.
Ni, Y.Q., Ye, X.W. and Ko, J.M. (2010), "Monitoring-based fatigue reliability assessment of steel bridges: analytical model and application", *J. Struct. Eng. - ASCE*, **136**(12), 1563-1573.
Ni, Y.Q., Ye, X.W. and Ko, J.M. (2012), "Modeling of stress spectrum using long-term monitoring data and finite mixture distributions", *J. Eng. Mech. - ASCE*, **138**(2), 175-183.
Ruan, J., *et al*. (2015), "An anti-noise real-time cross-correlation method for bolted joint monitoring using piezoceramic transducers", *Smart Struct. Syst*., **16**(2), 281-294.
Siu, S., *et al*. (2014), "Stress wave communication in concrete: I. Characterization of a smart aggregate based concrete channel", *Buiocontrol Sci. Technol*., **23**(12).
Song, G., *et al*. (2007), "Concrete structural health monitoring using embedded piezoceramic transducers", *Smart Mater. Struct*., **16**(4), 959-968.
Song, G., Gu, H. and Mo, Y.L. (2008), "Topical review: Smart aggregates: multi-functional sensors for concrete structures—a tutorial and a review", *Smart Mater. Struct*., **17**(3), 847-854.
Song, G., Olmi, C. and Gu, H. (2007), "An overheight vehicle bridge collision monitoring system using piezoelectric transducers", *Smart Mater. Struct*., **16**(2), 462-468.
Su, J.C. (2009), Survey on CFST arch bridges and research on their void problem, Southwest Jiaotong University, Chengdu, Sichuan, China.
Xiao, H., Zheng, J. and Song, G. (2016), "Severity evaluation of the transverse crack in a cylindrical part using a PZT wafer based on an interval energy approach", *Smart Mater. Struct*., **25**(3), 035021.
Xu, B., Chen, H. and Xia, S. (2017), "Numerical study on the mechanism of active interfacial debonding detection for rectangular CFSTs based on wavelet packet analysis with piezoceramics", *Mech. Syst. Signal Pr*., **86**, 108-121.
Xu, B., Chen, H. and Xia, S. (2017), "Study on the active debonding detection mechanism for circular CFSTs with PZT technology using wavelet packet analysis", *Smart Struct. Syst*., **19**(2), 181-194
Xu, B., *et al*. (2013), "Active interface debonding detection of a concrete-filled steel tube with piezoelectric technologies using wavelet packet analysis", *Mech. Syst. Signal Pr*., **36**(1), 7-17.
Xu, B., Li, B. and Song, G. (2012), "Active debonding detection for large rectangular CFSTs based on wavelet packet energy spectrum with piezoceramics", *J. Struct. Eng. - ASCE*, **139**(9), 1435-1443.
Yao, P., *et al.* (2016), "Structural health monitoring of multi-spot welded joints using a lead zirconate titanate based active sensing approach", *Smart Mater. Struct*., **25**(1), 015031.
Ye, X.W., Su, Y.H., Xi, P.S., Chen, B. and Han, J.P. (2016), "Statistical analysis and probabilistic modeling of WIM monitoring data of an instrumented arch bridge", *Smart Struct. Syst.*, **17**(6), 1087-1105.
Yi, T.H., Li H.N. and Gu, M. (2013), "Wavelet based multi-step filtering method for bridge health monitoring using GPS and accelerometer", *Smart Struct. Syst*., **11**(4), 331-348.
Yi, T.H., Li, H.N. and Wang, C.W. (2015), "Multiaxial sensor placement optimization in structural health monitoring using distributed wolf algorithm", *Struct. Control Health Monit.*, **23**(4), 719-734.
Zeng, L., *et al*. (2015), "Bond slip detection of concrete-encased composite structure using shear wave based active sensing approach", *Smart Mater. Struct*., **24**(12), 125026.
Zhang, L., *et al*. (2016), "Health monitoring of cuplok scaffold joint connection using piezoceramic transducers and time reversal method", *Smart Mater. Struct*., **25**(3), 668-671.
Zou, D., Liu, T., Huang, Y., Zhang, F., Du, C. and Li, B. (2014), "Feasibility of water seepage monitoring in concrete with embedded smart aggregates by P-wave travel time measurement", *Smart Mater. Struct*., **23**(6), 067003.
Zou, D., Liu, T., Huang, Y., Zhang, F., Du, C. and Li, B. (2014), "Feasibility of water seepage monitoring in concrete with embedded smart aggregates by P-wave travel time measurement", *Smart Mater. Struct*., **23**(6), 067003.
Zou, D., Liu, T., Qiao, G., Huang, Y. and Li, B. (2014), "An experimental study on the performance of piezoceramic-based smart aggregate in water environment", *IEEE Sens. J.*, **14**(4), 943-944.